

Supplementary Information

Production of Valuable Biopolymer Precursors from Fructose

Xuan Liu, Daniel Chee Yin Leong, and Yujie Sun*

Department of Chemistry, University of Cincinnati, Cincinnati, OH 45221, United States

*yujie.sun@uc.edu

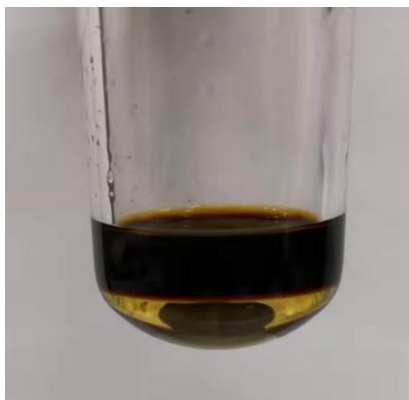


Figure S1. Photograph of reaction mixture after fructose dehydration. The reaction was performed with 100 wt% fructose and 10 mol% HCl at 140 °C in 1.5 mL sat. NaCl and 3 mL THF for 1 min.

Table S1. Results for HCl catalyzed fructose dehydration at 140 °C in 1.5 mL sat. NaCl and 3 mL THF.

Yield (%) Time Weight%	0.1 min	0.5 min	1.0 min	2.0 min
20	56	64	62	67
50	64	81	82	79
100	62	77	83	78
150	67	72	71	72
200	70	73	68	65

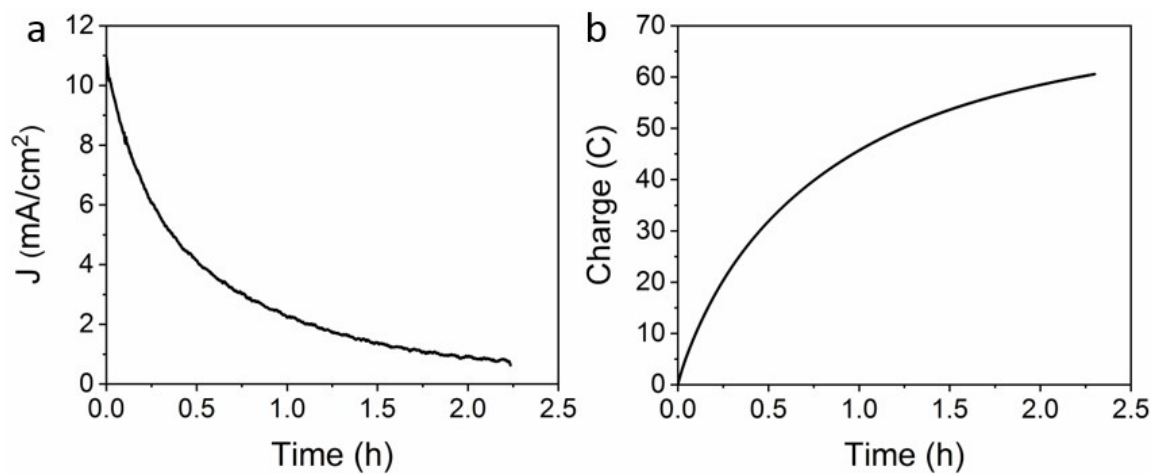


Figure S2. Chronoamperometric (a) and charge accumulation curve (b) of Ni/NF at 0.7 V vs. SCE in 1.0 M NaOH containing 10 mM fructose derived HMF.

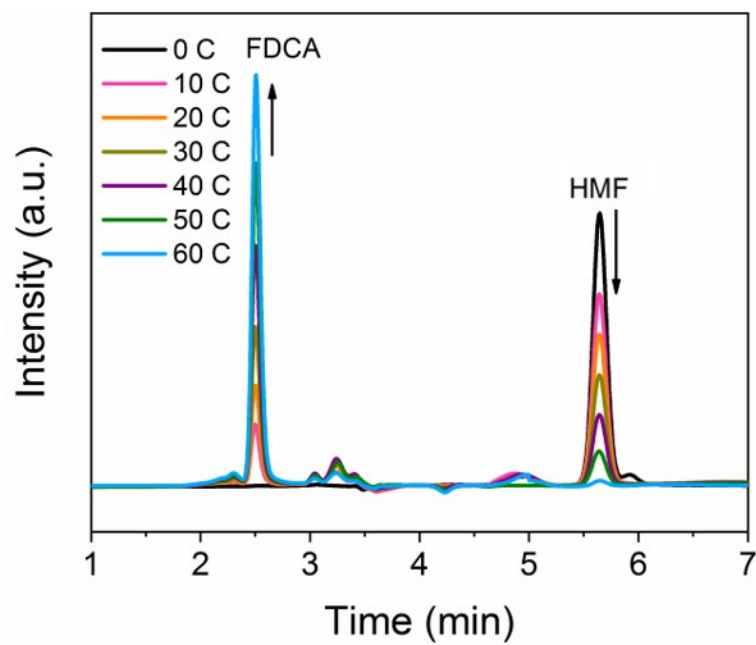


Figure S3. HPLC spectra of reaction mixtures during the electrolysis of 10 mM fructose derived HMF in 1.0 M NaOH at 0.7 V vs SCE.

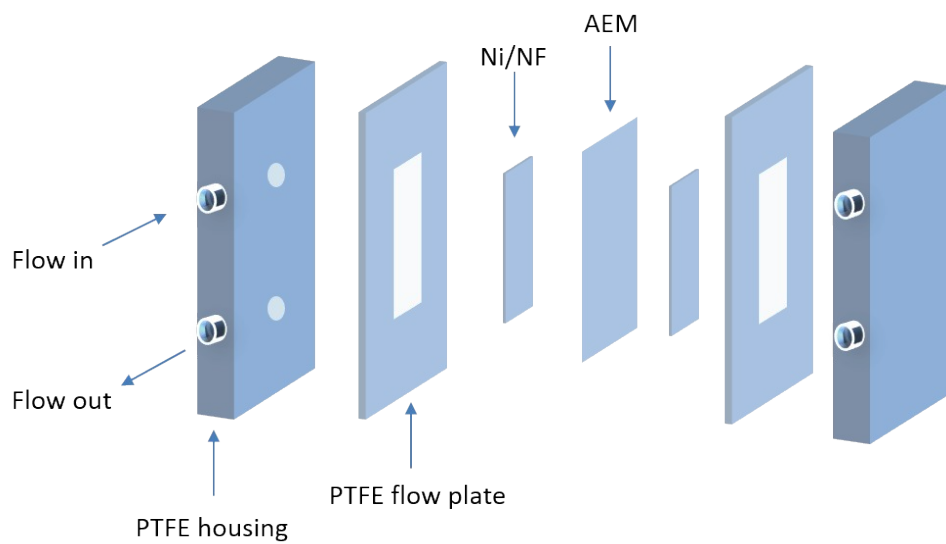


Figure S4. Diagram of the zero-gap membrane reactor used for flow electrolysis of HMF oxidation and reduction. The membrane electrode assembly comprises the cathode and anode on either side of the anion exchange membrane (AEM).

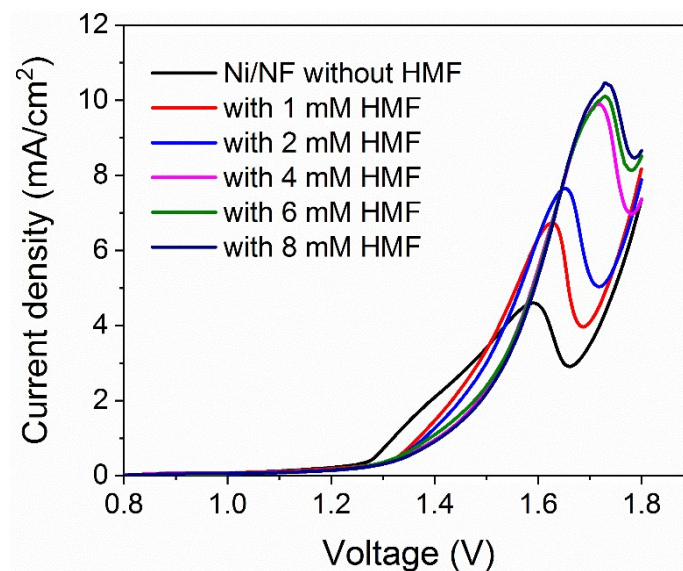


Figure S5. LSV curves of Ni/NF with different HMF concentrations in 1.0 M NaOH at a scan rate of 10 mV/s.

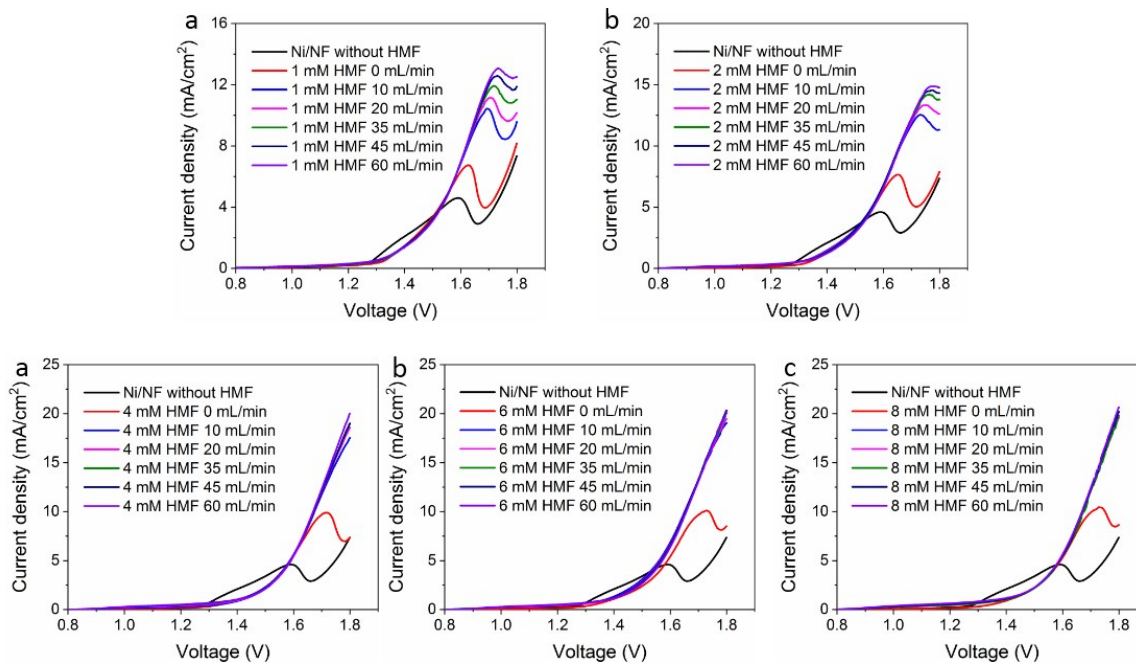


Figure S6. LSV curves of Ni/NF with different HMF concentrations and flow rates in 1.0 M NaOH at a scan rate of 10 mV/s.

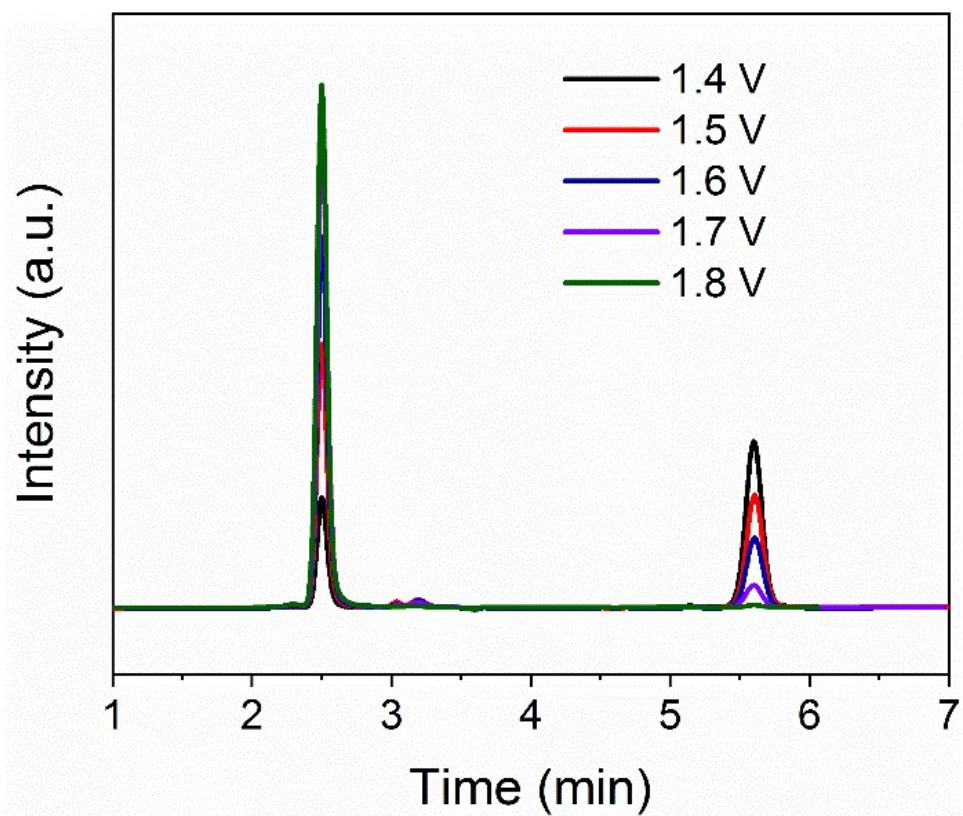


Figure S7. HPLC spectra of outlet electrolytes for flow electrolysis conducted at different applied voltages.

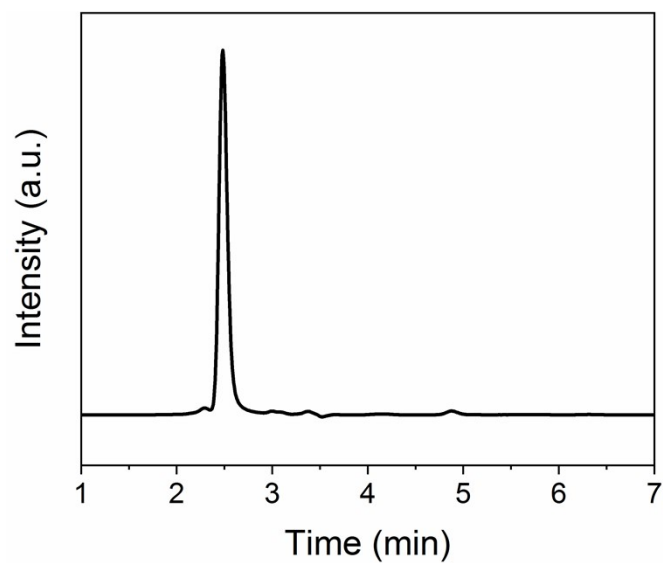


Figure S8. HPLC spectrum of outlet electrolyte for the flow electrolysis utilizing the reaction mixture after fructose dehydration in 1.0 M NaOH at 1.5 V with a flow rate of 2.8 mL/h. The electrode area was 28 cm².

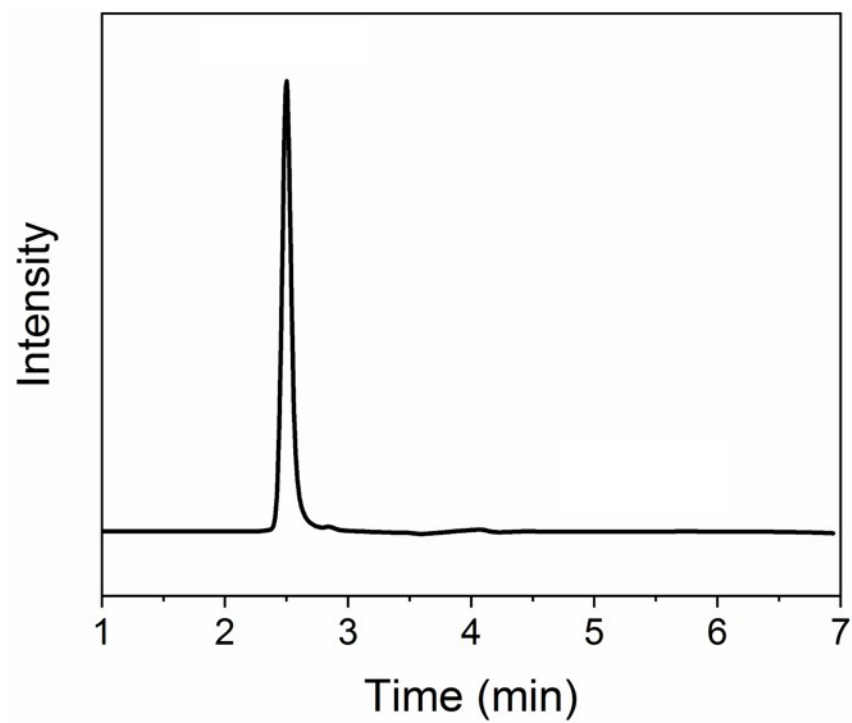


Figure S9. HPLC spectrum of outlet electrolyte for the flow electrolysis utilizing the reaction mixture after fructose dehydration at 1.8 V with a flow rate of 5 mL/h.

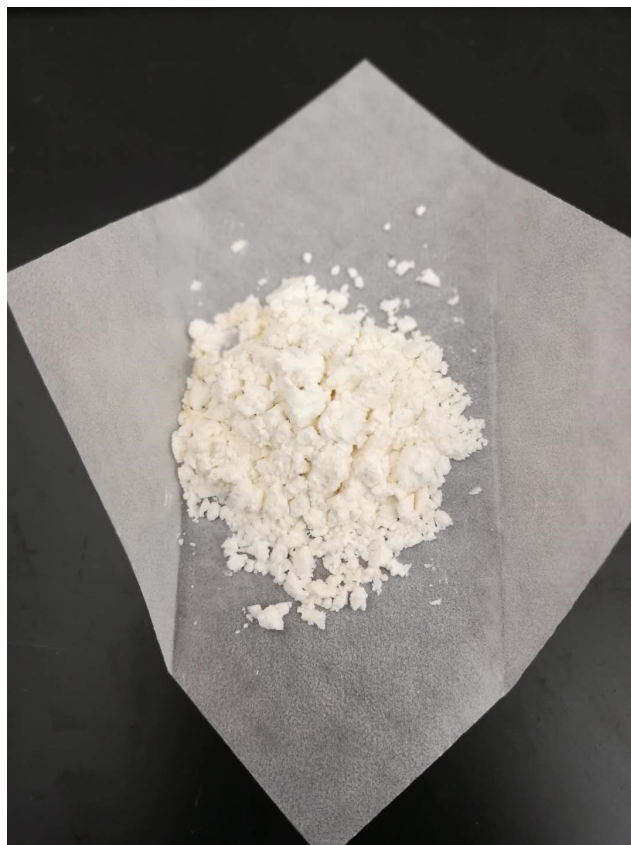


Figure S10. Photograph of obtained FDCA after electro-oxidation of fructose derived HMF.

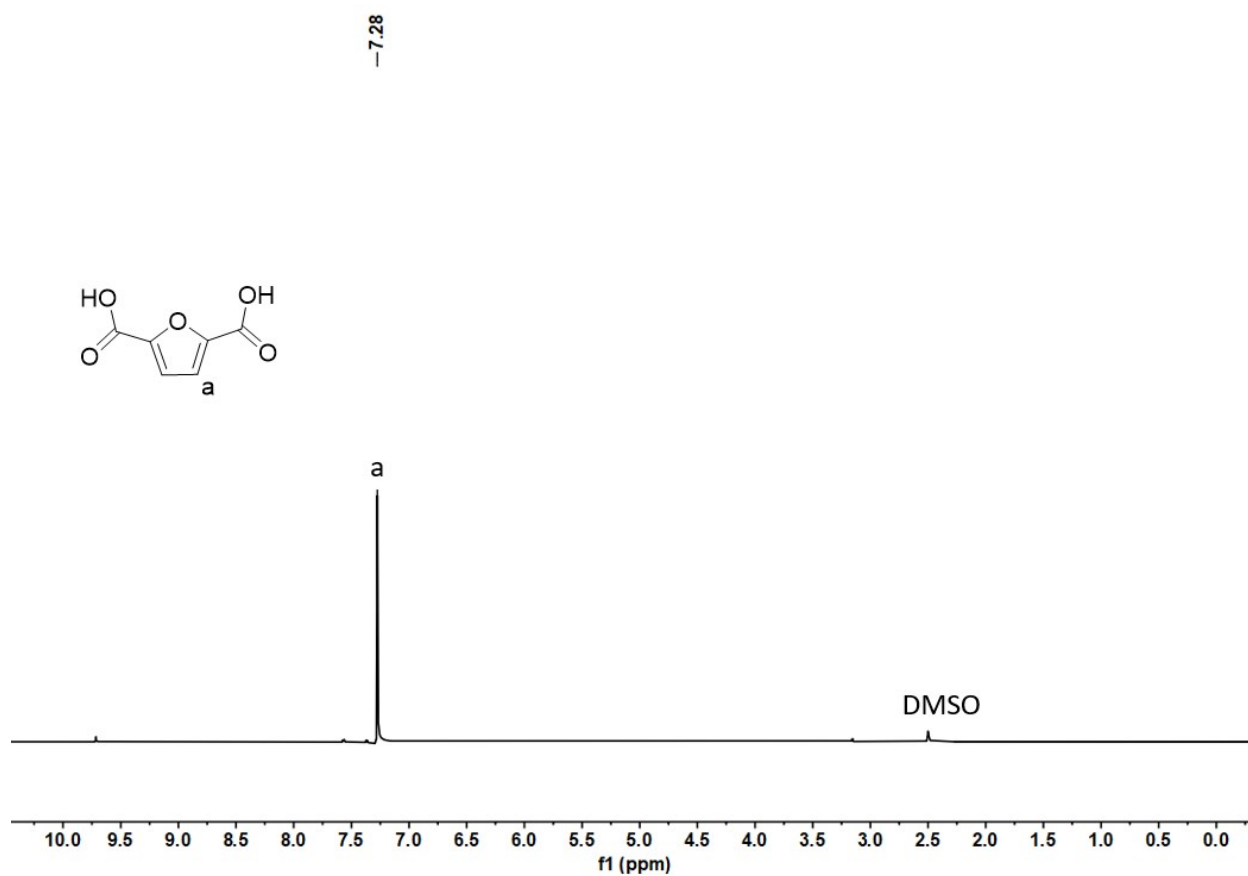


Figure S11. ^1H NMR spectrum (400 MHz, $\text{DMSO-}d_6$) of obtained FDCA after electro-oxidation of fructose derived HMF.

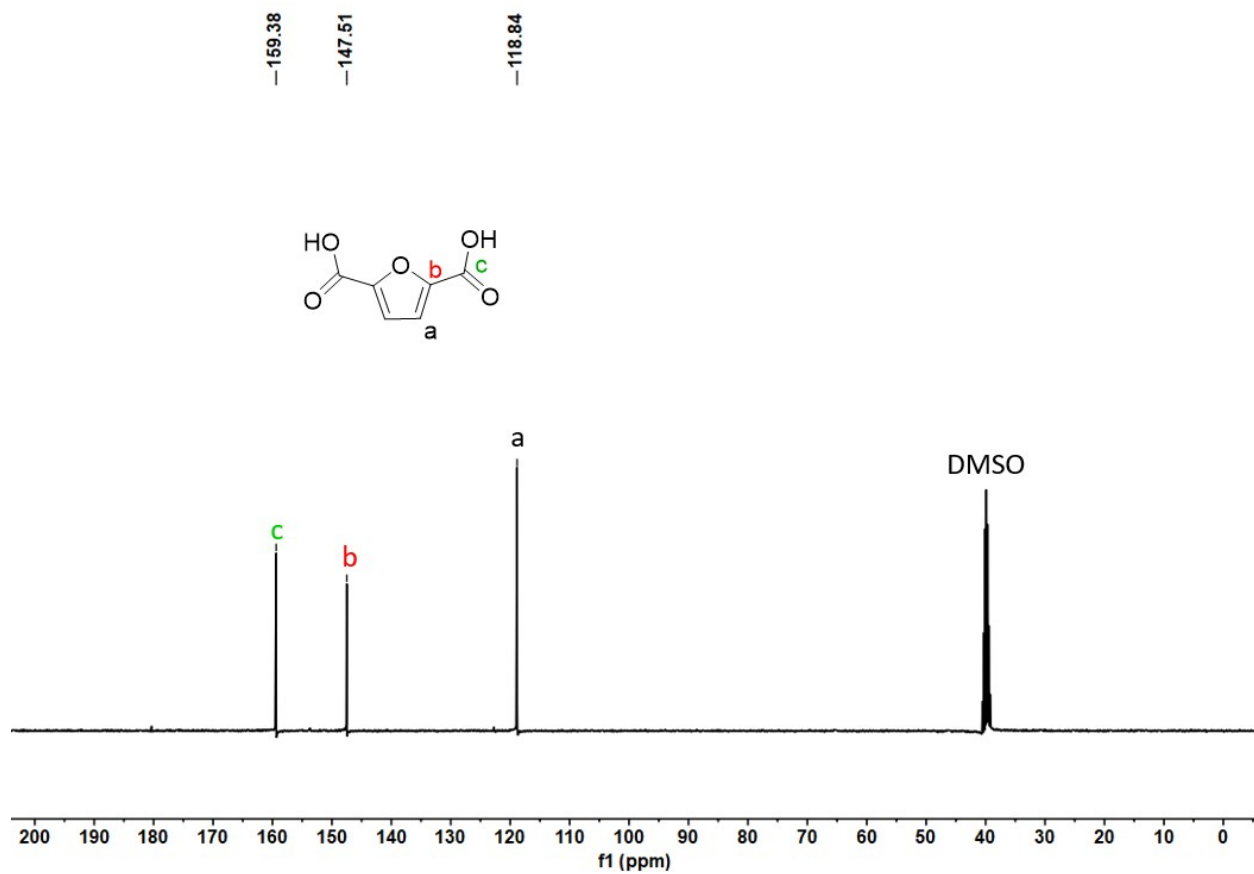


Figure S12. ¹³C NMR spectrum (400 MHz, DMSO-*d*₆) of obtained FDCA after electro-oxidation of fructose derived HMF.

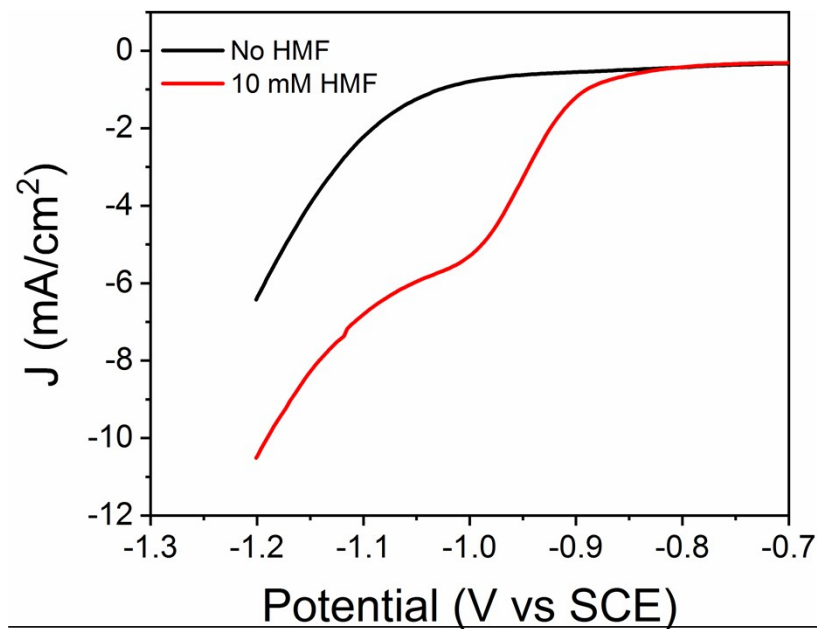


Figure S13. LSV curves collected on a Ag/Cu electrode in pristine 0.2 M borate buffer (pH 9.0) (black) and 0.2 M borate buffer containing 10 mM fructose derived HMF (red) (scan rate = 10 mV/s).

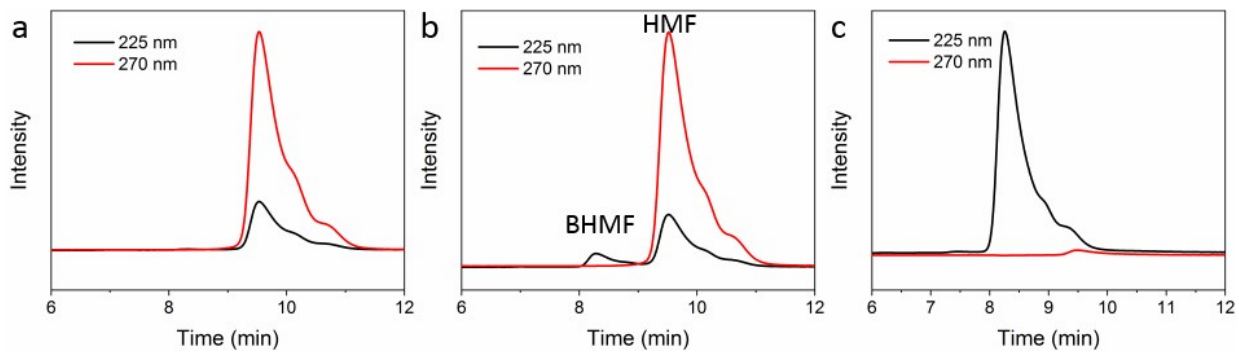


Figure S14. HPLC spectra of reaction mixtures at different potentials (a) -1.5 V, (b) -1.7 V, and (c) -1.9 V with a flow rate of 2 mL/h. Spectra collected at 225 nm and 270 nm were used to detect BHMF and HMF, respectively.

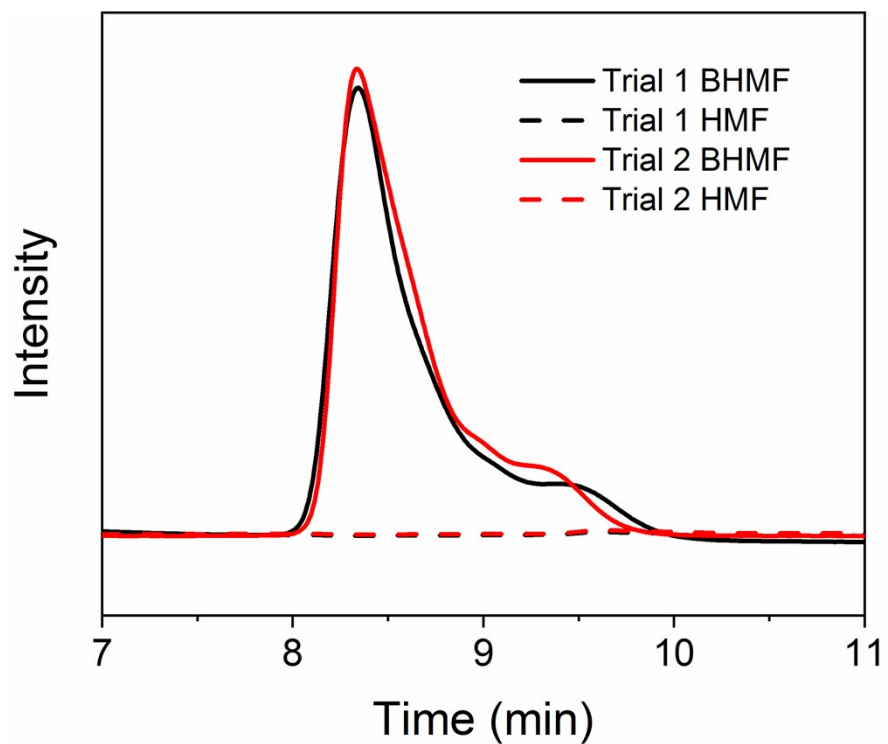


Figure S15. HPLC spectra of reaction mixtures of two individual electrolysis of fructose derived HMF at -1.9 V with a flow rate of 2 mL/h.

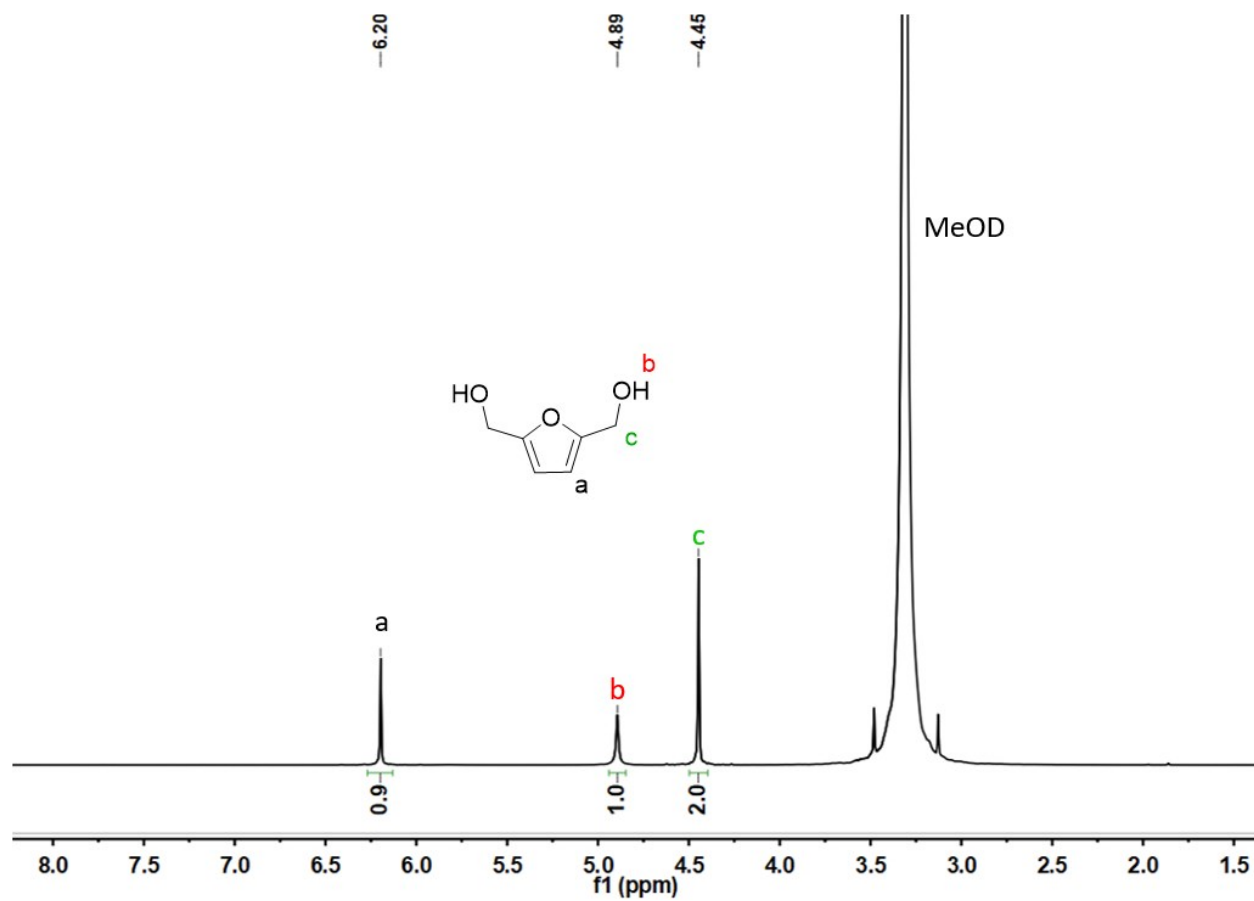


Figure S16. ^1H NMR spectrum (400 MHz, methanol- d_4) of obtained BHMf after electrohydrogenation of fructose derived HMF.

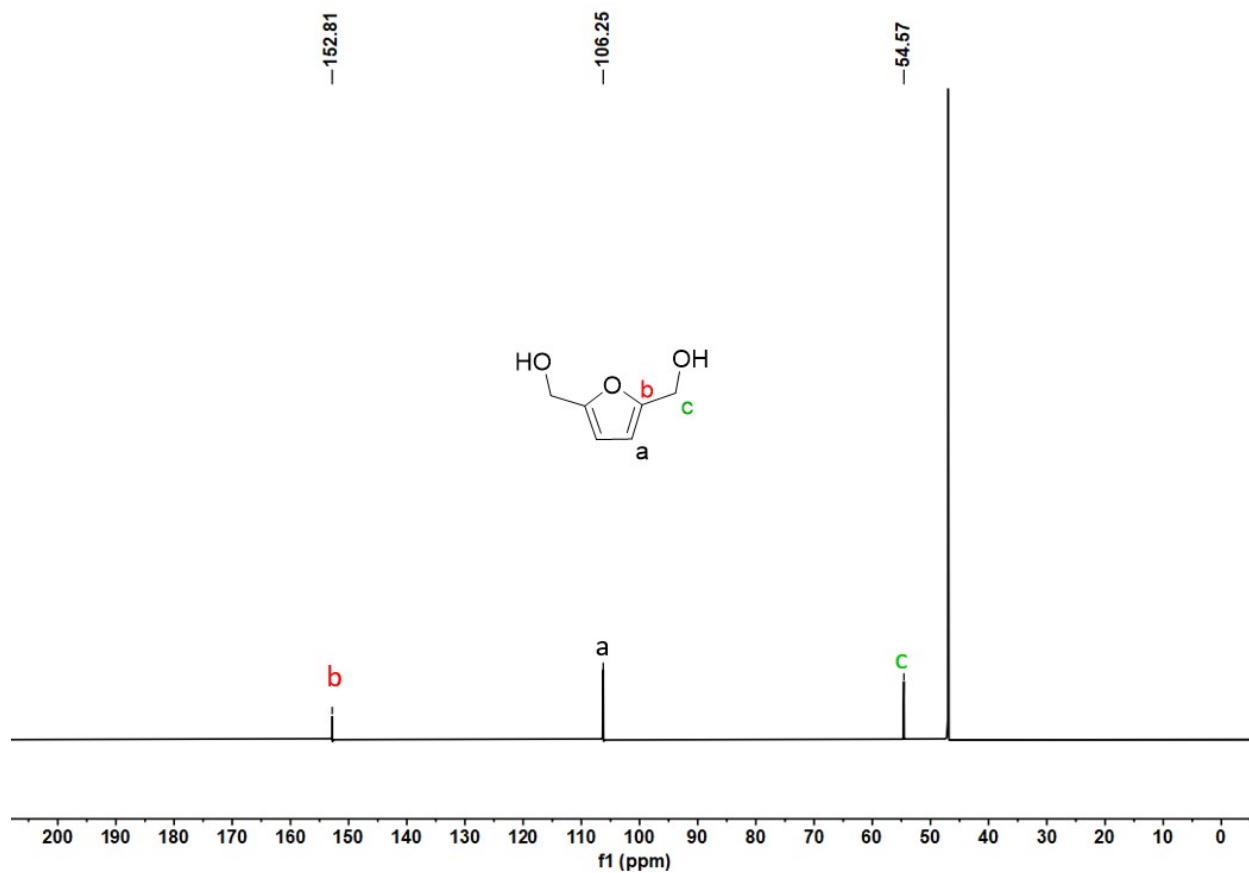


Figure S17. ^{13}C NMR spectrum (400 MHz, $\text{DMSO-}d_6$) of obtained BHMf after electrohydrogenation of fructose derived HMF.